Journal of Newviews in Engineering and Technology (JNET)
Vol 3, Issue 3, September 2021
Available online at http://www.rsujnet.org/index.php/publications/2021-edition
e- ISSN: 2795-2215

A Comparative Analysis and Simulation of the HVA Current and HVD Current connectivity of Bonny Island to the National Grid.

Dumkhana, L.[1], Ahiakwo, C. O.[2], Idoniboyeobu, D. C.[3], and Braide, S. L.[4]
Faculty of Engineering, Rivers State University, Port Harcourt, Rivers State, Nigeria.
les_dr@yahoo.com

ABSTRACT

The study presented a comparative analysis and simulation of high voltage alternating current and direct current transmission network (a case study of transmission network connectivity of Bonny Island to Afam independent power project (IPP), Rivers State, Nigeria. This objective was achieved by obtaining the necessary data on power transformer and the route length from Afam IPP generating station to Bonny Island, the transformer current, the transformer loading, the active power, the reactive power, the apparent power, the complex power, the power factor and the phase voltage on each transformer on the network, the busbar current, the cable size, conductor resistance, the cross sectional area of the conductor, the voltage drop on each Buses, and the resistance of line per Kilometer, the components of the HVDC link (the rectifier and the inverter) were determined. Voltage stability technique was use in implementing the HVAC and HVDC transmission network. Electrical Transient Analyzer Program (ETAP 19.0.1) simulation software was used in designing transmission network. Newton-Raphson method was utilized in the achievement of the optimal load flow analysis of the network. The comparative analysis of HVAC and HVDC transmission network were performed, which indicate that the HVDC transmission network had 0.629Mvar different from the HVAC on Bus6 and Bus7. In conclusion HVDC transmission network was better-off than the HVAC network for the connectivity of Bonny Island to the national grid.

KEYWORDS: Bus bar current, HVAC, HVDC, power transformer and Voltage stability technique.

Cite This Paper: Dumkhana, L., Ahiakwo, C. O., Idoniboyeobu, D. C., & Braide, S. L (2021). A Comparative Analysis and Simulation of the HVA Current and HVD Current connectivity of Bonny Island to the National Grid. *Journal of Newviews in Engineering and Technology*. 3(3), 84 – 95.

1.0 INTRODUCTION

The challenges associated with increased penetration of HVAC transmission, which may be mitigated using a variety of other technologies or practices, which included HVDC smart grid technologies, energy storage, or other flexible HVDC technologies (Oyedepo *et al.*, 2018). HVDC is mostly explored currently for transmission (or sub-transmission) grid networks, it is practicable and suitable for long-distance connections (Hocko *et al.*, 2020; Gamal *et al.*, 2016). In the perspective of Fulton and Skumanich (2012), HVDC transmission networks are experiencing a swift growth of penetration as compared to HVAC transmission networks from 2010 to the present day. Researchers Gamal *et al.*, (2016), said by 2030 grid integrated HVDC transmission network of about 16 GW was a national target for Saudi Arabia in particular. In the view of Singh *et al.* (2011) about 32% of the HVDC transmission line was targeted by the European Union by 2030. To achieve a higher level of penetration of the HVDC transmission network, the US Department of Energy (DOE) has targeted and projected 20% of electricity to be distributed from the HVDC transmission network by 2030 (U.S. Energy Information Administration, 2018). In support of this assertion, Makarov *et al.* (2019), recently opined that the use of an HVDC transmission network has increased rapidly and it is estimated that by the end of 2020, the total global bulk power transmitted on HVDC transmission network will reach 303 *GW*.

Makarov *et al.* (2019 indicated that the electricity transmitted by high voltage direct current

Journal of Newviews in Engineering and Technology (JNET)
Vol 3, Issue 3, September 2021
Available online at http://www.rsujnet.org/index.php/publications/2021-edition
e- ISSN: 2795-2215

(HVDC) line of about 750 KV-800 kV was generally efficient for high power transmission for a long-distance line. In Huri's theory (2012), the distance between the HVDC line is economically viable and technical for sustainable transmission network as compare to high voltage alternating current (HVAC) transmission line. According to Gamal *et al.* (2016), network connectivity with HVDC connectivity improves when the battery storage is connected at the end, dividing the MPPTs according to multiple DC / AC or DC-DC boosts converters employed for integrating HVDC transmission system. A distributed power distribution (DG) switch is equipped with electronic emulation control technology (GEC) with voltage support by the drop of Volt / VAR, low voltage (LVRT), and the small capacity as described by (Hosseini et al., 2011). Few related foreign studies do not focus on the Bipolar HVDC link configuration parameters as used in the present study. Objectives of the Research

The following objectives are considered to:

i. Obtain the necessary data on power transformer and the route length from Afam IPP generating station to Bonny Island.

ii. Determine the transformer current, the transformer loading, the active power, the reactive power, the apparent power, the complex power, the power factor and the phase voltage on each transformer on the network,

iii. Determine the Bus bar current, the cable size, conductor resistance, the cross-sectional area of the conductor, the voltage drops on each Buses, the resistance of line per Kilometer,

iv. Determine the components of the HVDC link,

v. Voltage Stability Technique was used in implementing the HVAC and HVDC transmission network linking Bonny Island to the national grid.

vi. Electrical transient analyzer program (ETAP 19.0.1) simulation software was used in designing the Afam Independent Power Project power station with HVAC and HVDC transmission network linking Bonny Island to the national grid,

vii. Newton-Raphson Method was used in achieving the optimal load flow analysis on Afam IPP generating station with HVAC and HVDC transmission network linking Bonny Island to the national grid, and

viii. Compare HVAC and HVDC transmission network performed.

In this research work the following research gap was discovered since no two submarine cable projects are identical. Each has to be designed to fulfil its purpose, taking into account transmission distance, water depth, sea currents, risks of damage, etc. The Bipolar HVDC link configuration parameters used in this research are different from the one used by other researchers and the transmission distance used in this research was also different.

2.0 MATERIALS AND METHOD

The materials used for HVAC and HVAC / HVDC connection are power supply, switching power supply, power line, HVAC transmission line, bus line, HVDC connection, single load, phase electricity, and GPS used to determine the length of network systems Figure 1 and Figure 2. The HVDC connection consists of a rectifier (convert alternating current to direct current) and an inverter (convert direct current to alternating current). Voltage stability technique was formulated and implemented with Newton-Raphson method for the performance study of the optimal load flow analysis on the network. Electrical Transient Analyzer Program (ETAP) simulation software was used to achieve the designed network.

Journal of Newviews in Engineering and Technology (JNET)
Vol 3, Issue 3, September 2021
Available online at http://www.rsujnet.org/index.php/publications/2021-edition
e- ISSN: 2795-2215

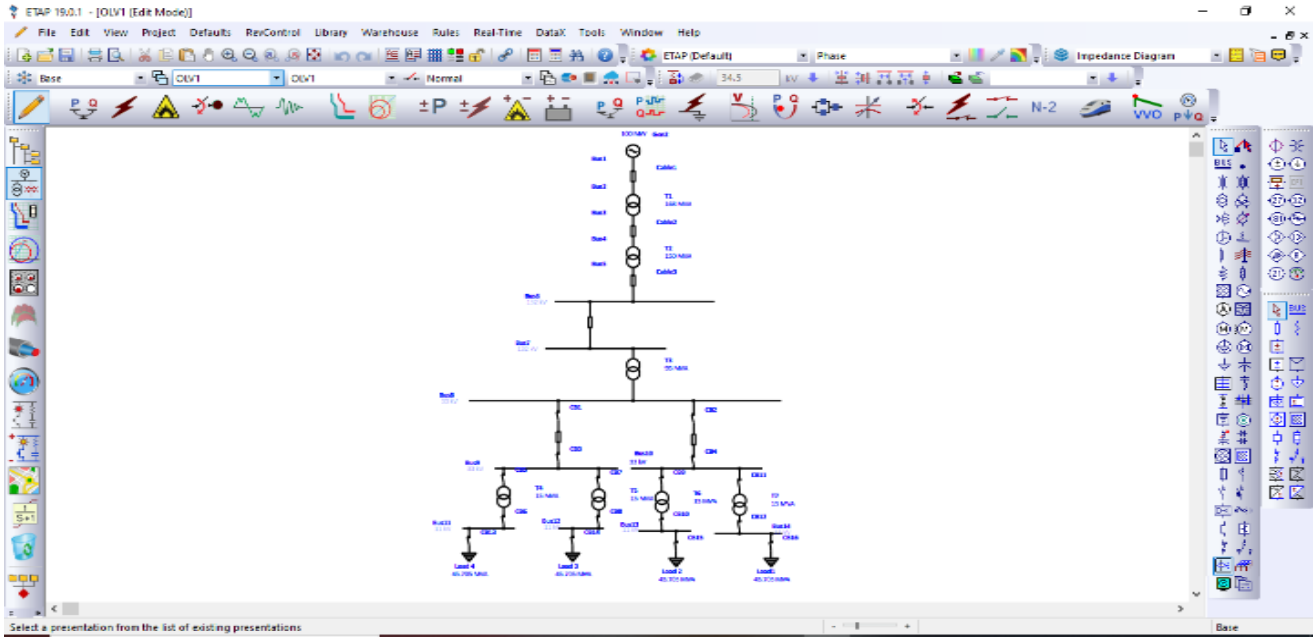

Figure 1: The Bonny Island HVAC Connected to Network National Grid

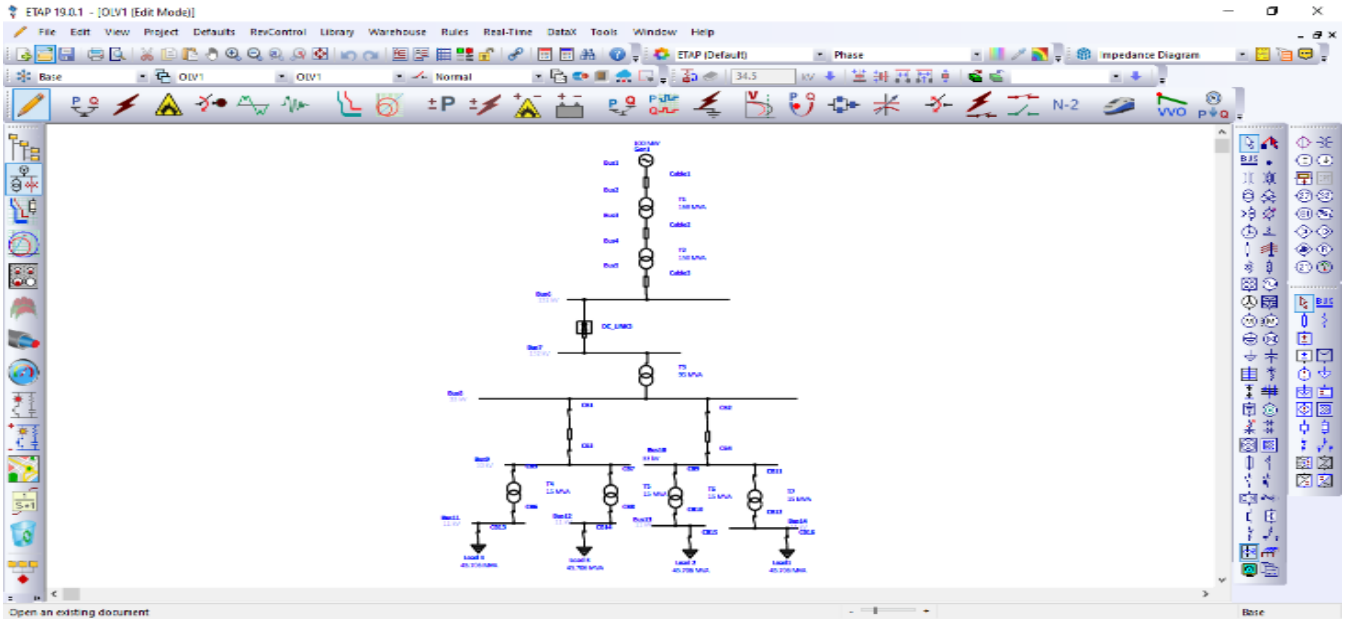

Figure 2: The Bonny Island HVDC Link Connected to Network National Grid.

Determination of the Generator Parameter

Determination of the Generator Real Power (MVA) on Network.

Converting the generator real power at 100MW to megavolt-ampere (MVA), the power factor of 0.85 was considered we have

$$MVA = \frac{MW}{pf} \quad (1)$$

Where, MW represent the megawatt value of the system and pf represents the power factor of 0.85 In determining the generator current on the network, the following formula were considered.

$$\text{Current } I = \frac{P(MVA)}{\sqrt{3}IV_L} \quad (2)$$

Journal of Newviews in Engineering and Technology (JNET)
Vol 3, Issue 3, September 2021
Available online at http://www.rsujnet.org/index.php/publications/2021-edition
e- ISSN: 2795-2215

Current with-it safety factor

$$I = \frac{P(MVA)}{\sqrt{3}V_L} \times Safety\ Factor$$

(3)

Inputting the Generator current values in (3) into (4) for determining the generator loading on the network, we have

Generator loading MVA= $\sqrt{3}IV_L$ (4)

Generator Active Power (MW) Determination on the Network

When you insert the generator control valve (4) into the input (5) to determine the power consumption of the generator,
we have.

Active power (MW)= $\sqrt{3}IV\cos\theta$ (5)

Generator Reactive Power (MVAR) Determination on the Network

Inputting the determine valve of generator loading in (4) into (6) to determine the generator active power on the network, we have

Reactive power (MVAR)= $\sqrt{3}VI\sin\theta$ (6)

The Determination of the Generator Apparent power in VA or MVA on the Network

Inputting the value of the active power (MW) and the reactive power (VAR or MVAR) in (5) and (6) into (7) in determining the value of the generator apparent power on the network, we have

Apparent power (MVA)= $\sqrt{\text{MW}^2 + \text{MVAR}^2}$ (7)

The Determination of the Generator Complex Power (S) on the Network.

The results are described by the generator used and the power generated by (8) to determine the generator in the network, we have

Complex power, $S = P + JQ$ (8)

Inputting the generator active power and generator reactive power value in (5) and (6) into (8) we have the determine value of the generator complex power.

The above procedure has been used to identify electron exchange targets.

The active power (MW) values and the apparent power (MVA) values on each transformer on the network were inputted into (9), to determine the power factor values on each transformer on the network, we have

Power factor, $\cos\theta = \frac{\text{Active power}}{\text{Apparent power}} = \frac{\text{MW}}{\text{MVA}}$ (9)

Determination of Phase Voltage

Equation (10) was used in determining the phase voltage on each transformer winding connected in star on the network as follows

Phase voltage $= \frac{\text{line voltage}}{\sqrt{3}}$

(10)

Determination of Bus Bar Current on the Network

Equation (2) was used in determining the Bus bar current on each Bus on the network.

Determination of Cable Size on the Network

The value of the cable should be 150% of the total load current (https://www.electrical4u.net/calculator/transformer-cable-size-calculations-calculator/).

Equation (11) was used in determining the cable size on the network, the transformer current values was divided by the multiplying factor of the cable.

Cable Size capacity $\boldsymbol{C_S = \frac{T_C}{C_{mf}}}$ (11)

Where, C_S represent the cable size, T_C represent the transformer current capacity and C_{mf} represent Multiplying factor

Determination of Conductor Resistance on the Network

Equation (12) was used in determining the resistance value on each Buses on the network, we have,

$R = \frac{V}{I}$ (12)

Determination of Conductor Cross Sectional Area on the Network

Equation (13) was used in determining the cross-sectional area of the conductor, we have

$R = \rho\frac{l}{A}\ \Omega/\text{km}$

(13)

Where: ρ is the resistance of the conductive material; l is its length in meters and A is the area of the material segment.

Journal of Newviews in Engineering and Technology (JNET)
Vol 3, Issue 3, September 2021
Available online at http://www.rsujnet.org/index.php/publications/2021-edition
e- ISSN: 2795-2215

$$A = \rho \frac{l}{R} \quad (14)$$

Determining the Voltage Drop along Each Buses

Equation (15) was used in determining the voltage drop in the conductor, we have

$$\text{voltage drop } V_d = \frac{(\sqrt{3} \times I_B \times (R\cos 0.8 + j \sin 0.6) \times Cable\ length \times 1.5)}{(Line\ Voltage \times \text{No of run} \cdot 1000)} \quad (15)$$

Determining Resistance of Line per Kilometer

Equation (13) was used in determining the resistance of line per Kilometer value of the route length of 58.6km linking Bonny Island to the national grid using the of 132KV Aluminium conductor steel reinforced (ACSR) resistivity value in table 1. Converting to meter, we have L = 58.6 × 10^3m, with cross-sectional area of 8.24×10^{-15} Ω·m since the main emphasis was on Bus 5, Bus 6 and Bus 7, we have

$$R = \rho \frac{l}{A} \Omega/\text{km}$$

Reactance of Line per Kilometer

$$X_o = 0.1445 log_{10} \frac{D_{GMD}}{r} + \frac{0.0157}{n} \Omega/\text{km}$$

(15)

Where n=3 (number of phases on the line)

Note that,

$D_{GMD} = 1.26$D, and the value of $D = 880$mm, $D = 0.88$m (horizontal space)

Since $D_{GMD} = 1.26$D, hence the value of D above was used to determine the geometric mean distance of conductor, has shown below

$D_{GMD} = 1.26$D, then $D_{GMD} = 1.26 \times 0.88 = 1.108$m

Hence, $D_{GMD} = 1.108$m

$$GMD = \sqrt[3]{D_{aa} \times D_{ab} \times D_{ac}} = 1.26D \quad 16)$$

$$r = \sqrt{\frac{A}{\pi}}$$

(17)

Where: A, represent the conductor cross sectional area of the aluminum conductor steel reinforced with galvanized, (A = 182mm2ACSR/GZ). GMD denotes the geometric mean distance m of the driver. r denotes the radius of the driver in meters (m). Although D is the distance between adjacent drivers (D = 0.88 m).

Calculation of Per Kilometer Inductive Reactance X,

$$X_o = 0.1445\ log_{10} \frac{1.108}{7 \times 10^{-8}} + \frac{0.0157}{n} \Omega/\text{km}$$

Multiply the route length of the Feeder with its inductive reactance.

Impedance of Line Per Kilometer

$$Z_o = R_o + JX_o$$

(18)

Admittance of Line Per Kilometer

$$Y_o = G_o + JB_o$$

(19)

Where; G_o represent the conductance of the line in Siemen's while B_o is the susceptance of the line in Siemens.

Equation (20) below was used in calculating the per kilometer capacitive susceptance B, we have

$$B = \frac{7.5}{log_{10}\left(\frac{D_{GMD}}{r}\right)} \times 10^{-6} \Omega/\text{km}$$

(20)

Multiply the route length, with its capacitive susceptance.

Using equation (14) above to determine the admittance (Y_o) of the network, we have

$$Y_o = G_o + JB_o$$

The HVAC transmission line consists of the inductance L, the shunt capacitance C for a given length, the operating voltage V and the current I. The power generated by the line is given as follows:

$$Q_c = \omega C V^2 \quad (21)$$

and consumer's reactive power

$$Q_c = \omega L I^2 \quad (22)$$

per unit length. If $Q_C = Q_L$

$$\frac{V}{I} = \left(\frac{L}{C}\right)^{1/2} = Z_s \quad (23)$$

Where Zs is the intersection of the lines.

The force carried by a line depends on the electrical conductivity and impact of the line (Meah & Sadrul, 2007)

$$.Z = VI = \frac{V^2}{Z_s} \quad (24)$$

The power flowing in the AC system and the power change in the line was expressed in (25)

Journal of Newviews in Engineering and Technology (JNET)
Vol 3, Issue 3, September 2021
Available online at http://www.rsujnet.org/index.php/publications/2021-edition
e- ISSN: 2795-2215

$P = \frac{E_1 E_2}{X} \sin \delta$ (25)

Where E1 and E2 are two final electric fields, δ is the phase difference between these electric fields and X is the resistance. The maximum transmission voltage occurs at δ = 90º and is correct

$P_{max} = \frac{E_1 E_2}{X}$ (26)

Where Pmax is the fixed limit.

Determination of Rectifier Capacity on the HVDC Link

Calculating the AC input current of the rectifier

$R_{IP} = I_L \times V_{DC}$ (27)

Where; R_{IP} is the AC input power of the rectifier, I_L is the line current and V_{DC} is the rectifier DC voltage value

Converting to MVA, we have

$R_{IP} = \frac{I_L \times V_{DC}}{1000000}$ KVA (28)

Converting (24) to Kilowatt, we have

$R_{KW} = R_{IP} \times P_F$ KW (29)

Determining the full power of the Rectifier

$R_P = \sqrt{3} * V_L * I_L * \cos\theta$ Watt (30)

Inputting the result in equation (30) into equation (31) to get Kilowatt, we have

$R_P = \frac{\sqrt{3} * V_L * I_L * \cos\theta}{1000}$ KW (31)

Determining the Output Power of the Rectifier

$R_{OP} = V_{DC} \times I_{DC_{OP}} \cos\theta$ (32)

Where; R_{OP} is the DC output power of the rectifier, $I_{DC_{OP}}$ is the DC line current of the rectifier and V_{DC} is the rectifier DC voltage value. Using the DC line current of the rectifier has the subject of the formula, we have

$I_{DC_{OP}} = \frac{R_{OP}}{V_{DC} \times \cos\theta}$ ADC (33)

Inputting the value of R_{OP} and V_{DC} in (32) into (34) into equation (34) to get the Rectifier output DC current.

Calculating the output power of the Rectifier, we have $AC_{PR} = \frac{DC_{PR}}{Eff}$ (34)

Where; AC_{PR} is the rectifier output power (AC), DC_{PR} is the rectifier input power (DC) and Eff is the efficiency of the rectifier.

Note that:

For we to determine the %loading of the rectifier will need to do some conversion, which are as follows.

Horse power (Hp) $H_P = K_w \times 746W$ (35)

Kilowatt power $KW_{pwr} = \sqrt{3} V_{FLC} I_{FLC} \times \cos\theta \times E_{ff} = DC_{pwr}$ (36)

$KW_{pwr} = DC_{pwr}$ (37)

That means,

$\sqrt{3} V_{FLC} I_{FLC} \times \cos\theta \times E_{ff} = \sqrt{3} V_{DC} I_{DC} \times \cos\theta$

Hence,

For the %loading of the rectifier will have

$E_{ff} = \frac{\sqrt{3} V_{DC} I_{DC} \times \cos\theta}{\sqrt{3} V_{FLC} I_{FLC} \times \cos\theta}$ (38)

$E_{ff} = \frac{\sqrt{3} V_{DC} I_{DC}}{\sqrt{3} V_{FLC} I_{FLC}}$ (39)

Determination of inverter Capacity on the HVDC Link

Note that, the output of the DC current of the rectifier is equal to the input value of the inverter power, so the result in equation (29) was taken has the inverter input, as follows

$I_{DC_{OP}} = \frac{R_{OP}}{V_{DC} \times \cos\theta}$ ADC

Where, $I_{DC_{ROP}}$ is the Rectifier output DC current and $I_{DC_{IIP}}$ is the Inverter input DC current

Calculating the inverter output current (AC), we have

$A_{PO_{Inv}} = \frac{R_{OP}}{V_{DC} Eff}$ Amp (40)

The value of the rectifier output power R_{OP} in (32) and the efficiency value in (39) was inputted into (28) to determine the output power of the inverter.

The %loading of the rectifier

The value of the rectifier output power in (32) and the value of the inverter output power in (40) into (41) in determining the efficiency of the inverter, we have

$A_{pwr} = \frac{DC_{pwr}}{EFF} \times 100$ (41)

Journal of Newviews in Engineering and Technology (JNET)
Vol 3, Issue 3, September 2021
Available online at http://www.rsujnet.org/index.php/publications/2021-edition
e- ISSN: 2795-2215

Determination of Static Load on the Network

The understanding of the energy for the electric field can be modeled as the static load in energy, the dependence of the load is usually ignored because the frequency change is usually constant to the limit. The standard measure of detail is a popular list of shipping agents and the model is as follows:

$$P = P_0 \times \left(\frac{V}{V_0}\right)^{\propto} \quad (42)$$

$$Q = Q_0 \times \left(\frac{V}{V_0}\right)^{\beta} \quad (43)$$

Where P and Q are the active and reactive powers consumed by the load at voltage V; P_0 and Q_0 are the active and reactive powers consumed by the load at voltage V_0; $\propto$ and β are the load exponents.

Minimum Complaints of the Power Flow Jacobian Matrix

The load flow of the equation can be expressed as follows

$$\begin{bmatrix}\Delta P\\ \Delta Q\end{bmatrix} = J\begin{bmatrix}\Delta\delta\\ \Delta V\end{bmatrix} \quad (44)$$

Where ΔP and ΔQ are variations of real and strong energy, respectively; Δδ and ΔV are the difference between the bus angle and the bus size, respectively.

Power Flow Jacobian matrix modal analysis If measurements are applied to reduce the flow rate of the Jacob matrix, the modal voltage change vector ν_m and the modal reactive power change vector q_m may be affected,

$$V_M = A^{-1}q_m \quad (45)$$

Where Λ = the line (λ1, λ2... λn) contains the eigenvalues of the reduced Jacobian matrix JR. If> i> 0, = i = 1... n, the system voltage is stable. If <i <0, the current for i is not constant, i = 1... n.

Effect of Load Modelling on the Voltage Stability Analysis of Simple 2-Bus System

$$P = -\left(\frac{EV}{X}\right)\sin\theta \text{ and} \quad (46)$$

$$Q = -\left(\frac{V^2}{X}\right) + \left(\frac{EV}{X}\right)\cos\theta \quad (47)$$

Case 1: Continuous power Let P_0 and Q_0 be the actual and strong power of bus-2 on the chassis or on the V0 power meter. The energy equivalent is:

$$P_0 = -\left(\frac{EV}{X}\right)\sin\theta \quad (48)$$

$$Q_0 = -\left(\frac{V^2}{X}\right) + \left(\frac{EV}{X}\right)\cos\theta \quad (49)$$

Rearranging and squaring the terms of the set of equations in (48) and (49), $V^4 + V^2(2Q_0X - E^2) + X^2\left(P^2{}_0 + Q^2{}_0\right) = 0$ (50)

To simplify the analysis, it is assumed that load power factor is constant, so that $\frac{Q_0}{P_0} = K$ (constant). Then, (50) becomes: $V^4 + V^2(2P_0KX - E^2) + X^2P^2{}_0(1 + K^2) = 0$ (51)

For real value of V, the necessary condition is that,

$$(2P_0KX - E^2) - 4X^2P^2{}_0(1 + K^2) \geq 0$$

$$P_0 \leq E^2(1 + K^2)^{\frac{1}{2}} - K \quad (52)$$

Equation (52) gives the power limit of the continuous power supply of the 2-bus system. There is no real solution for an electricity meter obtained above this load level, which is due to the fact that the system becomes electrically unstable after this load level.

Case 2:

Load current the ideal load current is determined by the relationships P = P_0 (V/V_0) and Q = Q_0 (V/V_0). To facilitate the analysis, the estimated voltage is 1 p.u., i.e., V_0 = 1. The energy transfer equation can be written as follows:

$$P_0V = -\left(\frac{EV}{X}\right)\sin\theta \quad (53)$$

$$Q_0V = -\left(\frac{V^2}{X}\right) + \left(\frac{EV}{X}\right)\cos\theta \quad (54)$$

Rearranging and squaring the terms in (53) and (54),

$$V^2 + 2Q_0VX + X^2\left(P^2{}_0 + Q^2{}_0\right) - E^2 = 0 \quad (55)$$

For real V, $(2Q_0X)^2 - 4\left(X^2\left(P^2{}_0 + Q^2{}_0\right) - E^2\right) \geq 0$

The above is equal to, $P_0 \leq E/X$, which is the potential limit if the final load is shorter. Therefore, there is almost no electrical effect on the load current.

Case 3: long load resistance

The ratio of the electric field to the positive constant current is P = P_0 (V/V_0) ^ 2 and Q = Q_0 (V/V_0) ^ 2. As in the previous case, V_0 has decided 1 pu and the energy is equal to the past

Journal of Newviews in Engineering and Technology (JNET)
Vol 3, Issue 3, September 2021
Available online at http://www.rsujnet.org/index.php/publications/2021-edition
e- ISSN: 2795-2215

impedance loads are $P = P_0\left(\frac{V}{V_0}\right)^2$ and $Q = Q_0\left(\frac{V}{V_0}\right)^2$. Similar to the previous case, V_0 was taken to be 1 p.u. and the power flow equations became

$$P_0V^2 = -\left(\frac{EV}{X}\right)\sin\theta \quad (56)$$

$$Q_0V^2 = -\left(\frac{V^2}{X}\right) + \left(\frac{EV}{X}\right)\cos\theta \quad (57)$$

Rearranging and squaring the terms in (56) and (57)

$$V^2\left(X^2\left(P^2{}_0 + Q^2{}_0\right) + 2Q_0X + 1\right) = E^2 \quad (58)$$

Whereby,

$$V = \left(\frac{E}{\left(X^2\left(P^2{}_0+Q^2{}_0\right)+2Q_0X+1\right)}\right)^{\frac{1}{2}} \quad (59)$$

3. RESULTS AND DISCUSSION:

The presentation of the HVAC optimal power flow of Bonny Island connectivity to the national grid result in Figure 3, shows that the network has one synchronous generator, seven transformers, fourteen Buses, two major transmission lines, and four static loads. The synchronous generator/power grid was rated at 100MW, 117.647MVA, 94.88%voltage, the operating Megawatt was 13.993MW with 85.56Mvar, it has 100% Bus nominal voltage with 85%PF and 95% efficient. The 168MVA transformer was used as step-up to 330kv line transmitted from Afam power station and was stepped down with 150MVA transformer at Bodo in Gokhana Local Government Area of Rivers State, which was transmitted with 132kv line from Bodo to Bonny waterside and was stepped down with 95MVA transformer at Bonny waterside, and was step down to 33kv line at Bonny Island with 15MVA transformer, the 15MVA transformer further stepped it down 11kv line connected to the 45.705MVA static load with the rated values of (7.999MW, 45Mvar, 2399Amps and 17.5%PF). The designed loading of the four static load rating was 100%. The load was 7.917MW, 44.543Mvar and the feeder loss was 0.555MW and 0.133Mvar which was 100% normal, respectively. In summary the total generation was 13.993MW, 85.565Mvar, 86.702MVA and 16.14% PF Lagging. While the total loading and demand was 7.999MW, 44.977Mvar, 45.682MVA and 17.51 %PF Lagging.

The Presentation of HVDC Optimal Power Flow of Bonny Island Connectivity

The configuration of the synchronous generator, transformers and static loads in figure 4, were repeated all the same with the configuration in figure 4, except the HVDC link between Bus6 and Bus7.

The Bipolar HVDC link between Bus6 and Bus7 shows that 132kv line with 50Hz was used as the rectifier input, while 132kv was used in connecting the primary and the secondary side of the rectifier transformer, the 150MVA transformer has 5% tap, same configuration was used for the inverter input and the inverter transformer, as shown in figure 5.

The Different between HVAC and HVDC Link Connectivity.

The HVDC transmission network had 0.629Mvar different from the HVAC on Bus6 and Bus7, which indicates that HVDC transmission network was better-off than the HVAC transmission network.

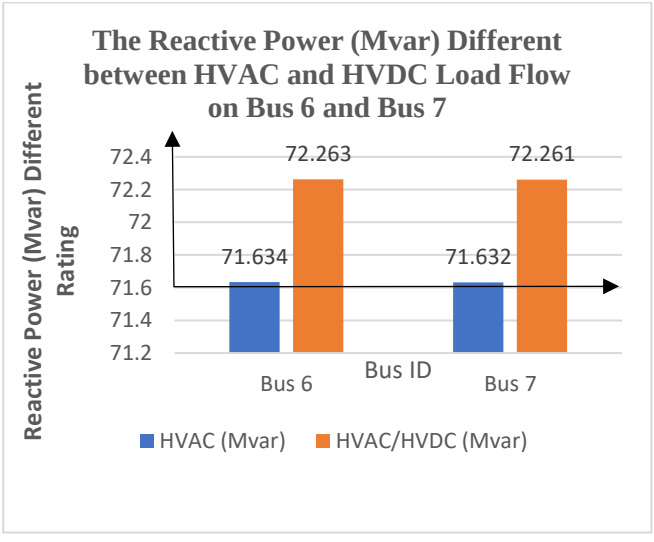

Figure 6: The Reactive Power (Mvar) Different between HVAC and HVDC Load Flow on Bus 6 and Bus 7.

Journal of Newviews in Engineering and Technology (JNET)
Vol 3, Issue 3, September 2021
Available online at http://www.rsujnet.org/index.php/publications/2021-edition
e- ISSN: 2795-2215

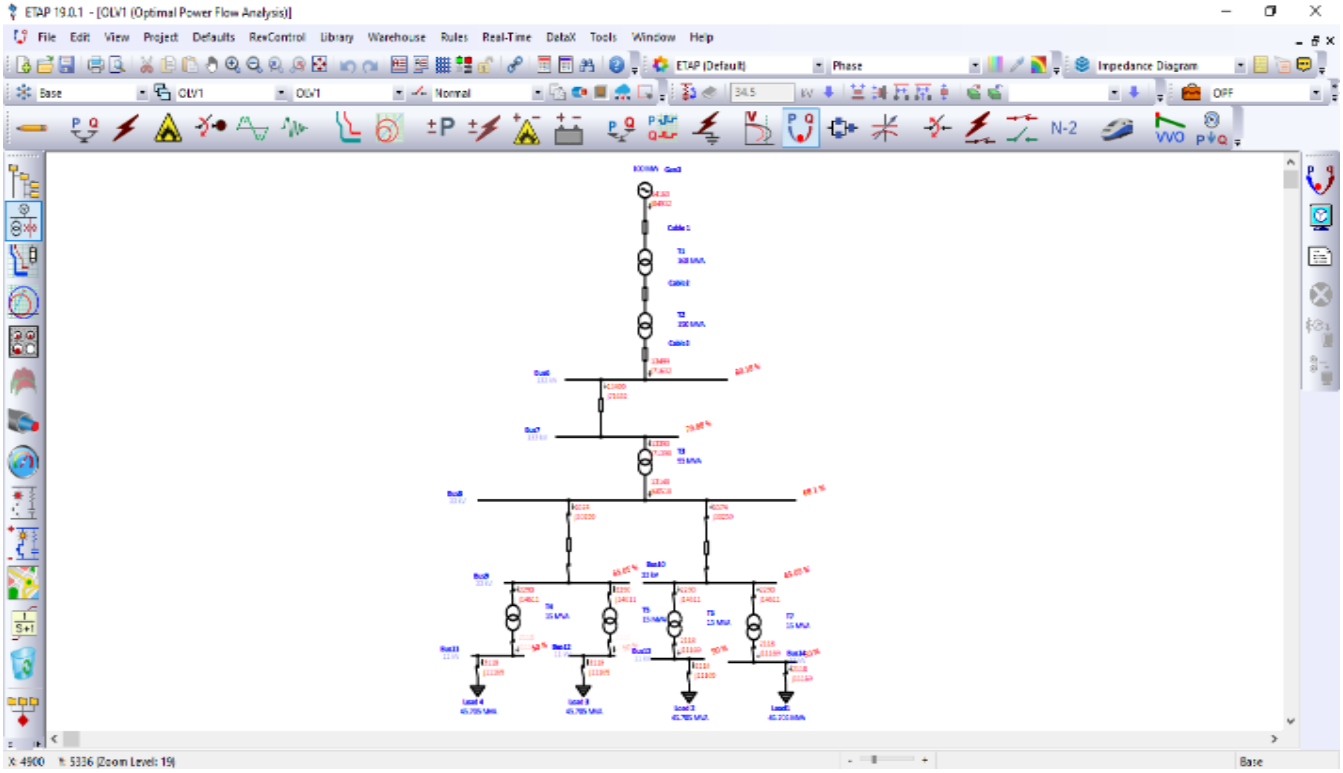

Figure 3: The HVAC Optimal Power Flow of Bonny Island to the National Grid

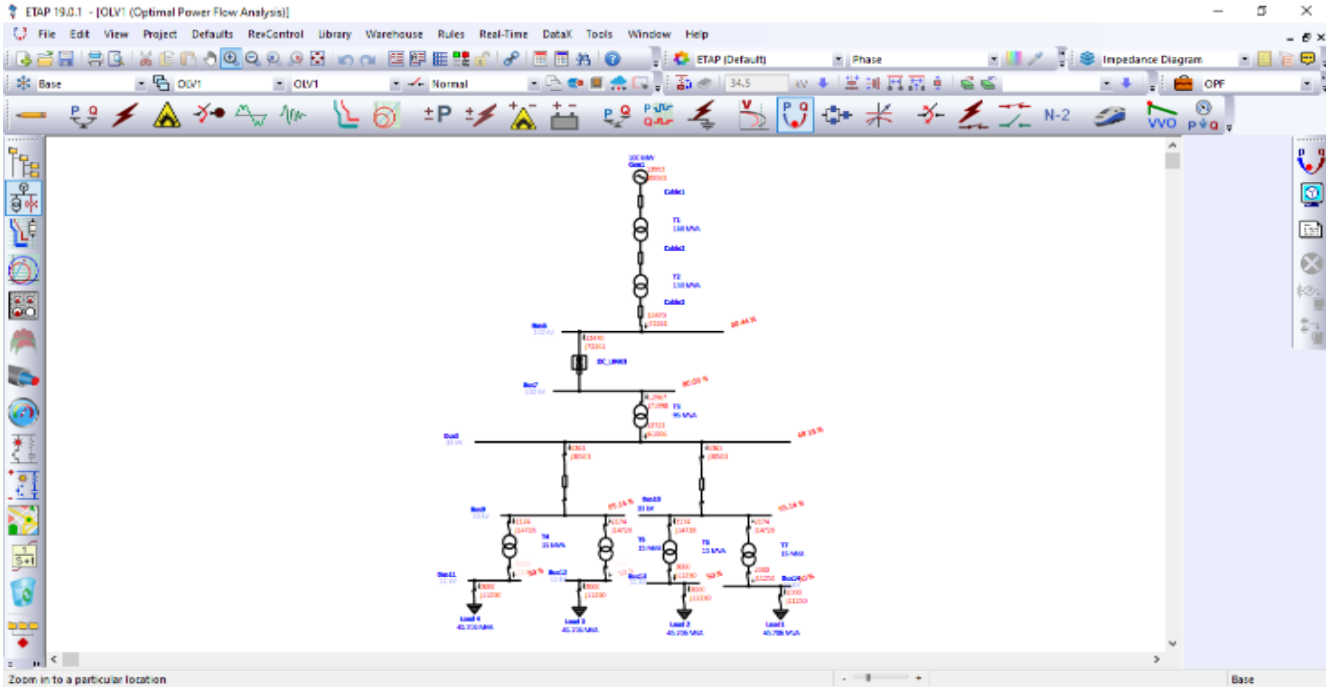

Figure 4: The HVDC Optimal Power Flow of Bonny Island to the National Grid

Journal of Newviews in Engineering and Technology (JNET)
Vol 3, Issue 3, September 2021
Available online at http://www.rsujnet.org/index.php/publications/2021-edition
e- ISSN: 2795-2215

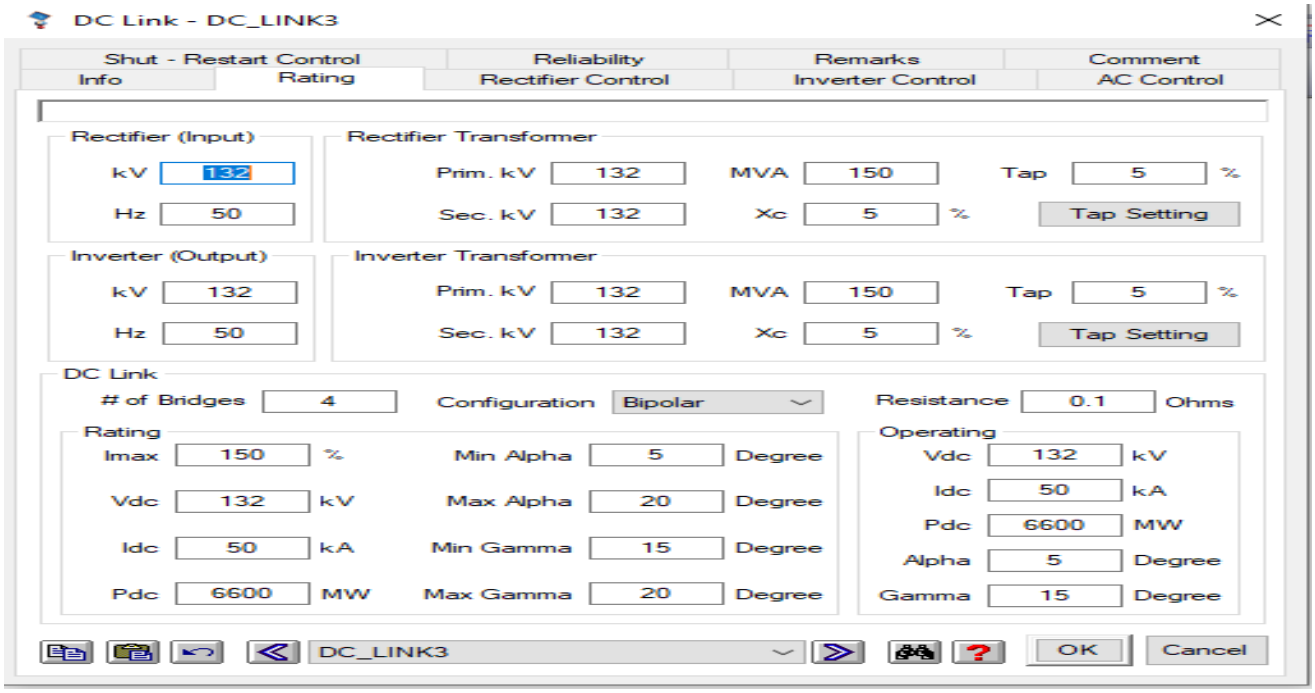

Figure 5: The HVDC Link Configuration

The Different between HVAC and HVDC Link Connectivity.

The HVDC transmission network had 0.629Mvar different from the HVAC on Bus6 and Bus7, which indicates that HVDC transmission network was better-off than the HVAC transmission network.

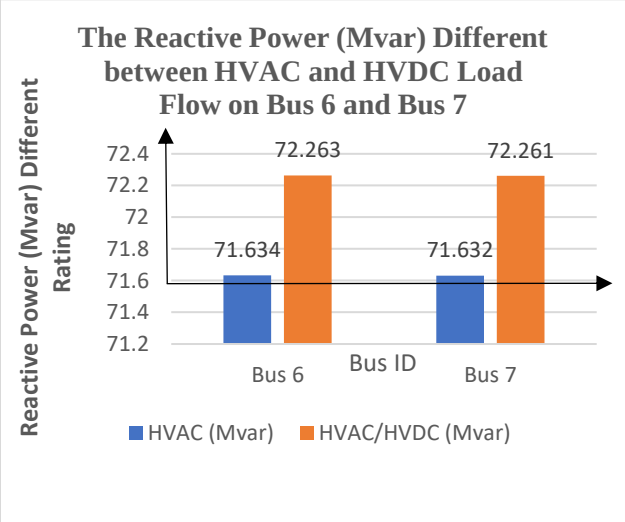

Figure 6: The Reactive Power (Mvar) Different between HVAC and HVDC Load Flow on Bus 6 and Bus 7.

The result in Figure 7, indicates that the reactive power on HVDC network has 0.325Mvar different from that of the HVAC network on Bus 11, Bus 12, Bus 13 and Bus 14

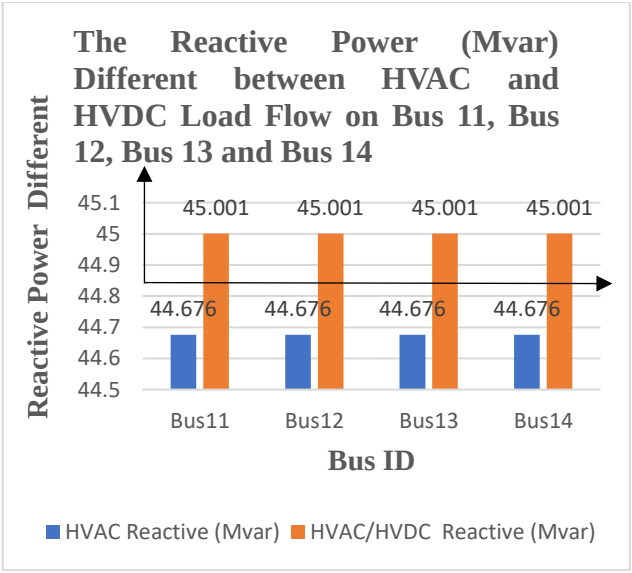

Figure 7: The Reactive Power (Mvar) Different between HVAC and HVDC Load Flow on Bus 11, Bus 12, Bus 13 and Bus 14.

The difference between HVAC and HVDC reactive power load flow on the network, indicates that the HVDC had a better performance than that

Journal of Newviews in Engineering and Technology (JNET)
Vol 3, Issue 3, September 2021
Available online at http://www.rsujnet.org/index.php/publications/2021-edition
e- ISSN: 2795-2215

of the HVAC network with a different of 0.633Mvar on Bus 2, 0.764Mvar on Bus 3, 0.7Mvar on Bus 4 and Bus 5 respectively, 0.629Mvar on Bus 6 and Bus 7 respectively, 0.6Mvar on Bus 8, 0.244Mvar on Bus 9 and Bus 10 respectively, 0.117Mvar on Bus 11, Bus 12, Bus 13 and Bus 14 respectively.

The difference in voltage percentage margin between HVDC and HVAC on the network, indicates that the voltage percentage margin on the HVDC network has a better performance than that of the HVAC network with a different of 0.168 % on Bus 1, 0.336 % on Bus 2, 0.3 % on Bus 3, 0.299 % on Bus 4, Bus 5 and Bus 6 respectively, 0.153 % on Bus 7, 0.076 % on Bus 8, 0.095 % on Bus 9 and Bus 10 respectively, while Bus 11, Bus 12, Bus 13 and Bus 14 had equal voltage percentage margin of 50 %, respectively.

The percentage power factor load flow difference between HVDC and HVAC network, indicates that the percentage power factor load flow on HVDC has a better performance than that of the HVAC network with a different of 0.3 %pf on Bus 2, 0.2 %pf on Bus 3, 0.1 %pf on Bus 4 and Bus 5 respectively, 0.2 %pf on Bus 6 and Bus 7 respectively, 0.8 %pf on Bus 8, 0.8 %pf on Bus 9 and Bus 10 respectively, 0.9 %pf on Bus 11, Bus 12, Bus 13 and Bus 14 respectively.

The design and nominal (loading, real power load, reactive power and feeder loss) on HVDC and HVAC Network, indicates that 100% design and Nominal Loading was on both the HVAC and HVDC network. The design and Nominal real power load on Bus 11, Bus 12, Bus 13 and Bus14 was 7.917MW respectively on both the HVAC and the HVDC network. The design and Nominal reactive power load on Bus 11, Bus 12, Bus 13 and Bus14 was 44.543 Mvar respectively on both the HVAC and the HVDC network. The design nominal feeder loss on Bus 11, Bus 12, Bus 13 and Bus14 was 0.555MW respectively on both the HVAC and the HVDC network.

4. CONCLUSION

In conclusion, the comparative analysis and simulation of the HVAC and HVDC connectivity of Bonny Island to the national grid were achieved by obtaining the necessary data on power transformer and the route length of the network, the transformer current, the transformer loading, the active power, the reactive power, the apparent power, the complex power, the power factor and the phase voltage on each transformer on the network, the Bus bar current, the cable size, conductor resistance, the cross sectional area of the conductor, the voltage drop on each Buses, and the resistance of line per Kilometer, the components of the HVDC link (the rectifier and the inverter) were also determined using voltage stability technique was used in implementing the Afam IPP generating station with HVAC and HVDC transmission network linking Bonny Island to the national grid for analysis. Electrical transient analyzer program (ETAP 19.0.1) simulation software was used in designing the Afam IPP generating station with HVAC and HVDC transmission network linking Bonny Island to the national grid. The comparative performance of the HVAC and HVDC transmission network were also accomplished. The comparative analysis of HVAC and HVDC transmission network were performed, which showed that the HVDC transmission network had 0.629Mvar different from the HVAC on Bus6 and Bus7, indicating that HVDC transmission network was better-off than the HVAC to be used for the transmission of electric bulk power to Bonny Island.

REFERENCES

Chinthavali, M., Debnath, S., Mohan, N., Hess, W., Duebner, D., Orser, D., Brown, H., Osborn, D., Feltes, J., Kurthakoti, D. C., & Zhu, W (2017). *Models and methods for assessing the value of HVDC and MVDC technologies in modern power grids*. Annual report July 2017.

Fulton S, & Skumanich A. (2012). New growth markets for PV: Micro-grids in developing countries - A case study. Proceedings of the 38th IEEE Photovoltaic Specialists

Conference (PVSC) (3303-3306) Austin, USA.

Gamal S., Tamer, K & Raed, S. (2016). Grid integration of large pv power systems using HVDC Link. *Int. Journal of Engineering Research and Application*, 6(9), 68-76.

Hocko P., Novak, M., Kolcun, M., & Conka, Z. (2020). Influence of photovoltaic power plants on the power system to the prediction for year 2020. Proceedings of the 14th Environment and Electrical Engineering Conference (EEEIC) (116-121). Krakow, Poland.

Hosseini, S., Nejabatkhah, F., Danyali, S., & Kh, S. (2011). Grid-Connected three-input PV/ FC/ battery power system with active power filter capability. Proceedings of the International Conference and Exhibition on Innovative Smart Grid Technologies (1-7) Manchester, United Kingdom

Hur, D. (2012). Economic considerations underlying the adoption of HVDC and HVAC for the connection of onshore wind farm in Korea. *J. Electr. Eng. Technol*. 7, 157–162.

Makarov, Y. V., Elizondo, M. A., O'Brien, J. G., Huang, Q., Kirkham, H., Huang, Z., …, Moduo, Y. (2019). Technical and economic assessment of VSC-HVDC transmission model: A case study of south-western region in Pakistan. Retrieved from www.mdpi.com/journal/electronics

Oyedepo, S. O., Babalola, O. P., Nwanya, S. C., Kilanko, O., Leramo, R. O., Aworinde, A. K., …, Agberegha, O. L. (2018). Towards a sustainable electricity supply in Nigeria: The role of decentralized renewable energy system. *European Journal of Sustainable Development*. 2(4), 40-58.

Singh D, Sharma N, Soo Y, & Jarial R. (2011). Global status of renewable energy and market: Future prospectus and target. Technical report of the Sustainable Energy and Intelligent Systems Conference (SEISCON) (171-176), Chennai, India.

U.S. Energy Information Administration (2018). Assessing HVDC transmission for impacts of non-dispatchable generation. *Independent Statistics & Analysis.* Retrieved from www.eia.gov